Journal of Alloys and Compounds 495 (2010) 316–318

Contents lists available at ScienceDirect

Journal of Alloys and Compounds

journal homepage: www.elsevier.com/locate/jallcom

Glass formation of alloys selected by lambda and electronegativity criteria in the Ti–Zr–Fe–Co system

M.F. de Oliveira[a,*], F.S. Pereira[a], B.T. Ramasco[b], C.S. Kiminami[b], W.J. Botta[b], C. Bolfarini[b]

[a] Universidade de São Paulo, EESC, SMM - Av. Trabalhador São Carlense, 400 - São Carlos, SP, 13566-590, Brazil
[b] Universidade Federal de São Carlos, DEMa - Rod. Washington Luiz, Km 235, São Carlos, SP, Brazil

ARTICLE INFO

Article history:
Received 3 July 2008
Received in revised form 27 October 2009
Accepted 28 October 2009
Available online 5 November 2009

Keywords:
Metallic glasses
Rapid-solidification
Amorphisation

ABSTRACT

This work evaluates the glass formation of selected alloys based on the Ti–Zr–Fe–Co system, assuming the synergy of two distinct criteria: minimum topological instability and average electronegativity plots. Combining the minimum topological instability and the average electronegativity values result in a plot in which the most probable good glass former compositions are identified. Ti–Zr rich alloys with Fe and Co additions were produced, compared against the final plot, and the best glass forming alloy composition was found to be very close the theoretically predicted ones on the Ti–Zr rich side, for both Ti–Zr–Fe and Ti–Zr–Co systems.

1. Introduction

In the last few years, many Ti-based alloy compositions with good glass forming ability (GFA) have been produced and received attention due to their potential properties for practical applications [1–3]. The first rapidly quenched alloys, in systems such as Ti–Ni–Si [4,5], Ti–Si [6], Ti–Be [7], Ti–Be–Si [8], Ti–Zr–Be [9] and Ti–(Fe, Co, Ni)–B [10], presented yield stresses of up to 2200 MPa, which are much higher than the corresponding values for typical commercial Ti-based alloys in the range of 1000 MPa.

The selection of good glass forming compositions, however, is not a trivial task and many groups work on models and theoretical approximations in order to predict, or at least guide, the laborious and expensive pinpointing of compositions in a given system.

The glass forming ability (GFA) of a given alloy composition can be defined as the inverse of the critical cooling rate necessary to avoid crystallization, the lower the critical cooling rate the higher the glass forming ability. From a practical point of view the GFA can be evaluated by the thickest fully amorphous sample that one can obtain by chill casting. If convection is not considered, the cooling rate is limited by thermal conduction in the liquid, which scales with the square of the sample thickness.

In the present work, the easy glass forming alloy compositions were selected based on two distinct criteria, minimum topological instability and average electronegativity plots, assuming a synergistic effect.

The background behind the minimum topological instability plot is the work of Egami and Waseda [11], which was later extended to predict the crystallization behavior of Al-rich amorphous alloys [12]. The same principle can be applied for intermetallic phases in order to find the best glass forming compositions in binary and ternary Cu–Zr-based alloys [13]. The topological instability parameter, λ, is defined as

$$\lambda \cong \sum_{i=1}^{n} \chi_i \left| \frac{Vm_i}{Vm_0} - 1 \right| \qquad (1)$$

which is an approximation of the original equation [12]. In Eq. (1) χ_i is the molar fraction of any of all n solute elements (denoted by i) in a given stoichiometric compound, Vm_i is the molar volume of such solute elements, and Vm_0 is the molar volume of the compound. The topological instability is related to the strain caused by solute atoms in a crystalline matrix. Increasing the atomic radius mismatch, or the solute concentration, the introduced strains become so high that the system must change the topology and break its long range ordering in order to better accommodate the atoms. At this point, if the cooling rate of a liquid is high enough to avoid solute segregation, the amorphous phase appears as a competitive phase against crystallization. It is important to point out that Eq. (1) can lead to some errors when the packing factors of elements and compounds differ too much. Refer to [13] for further details.

The larger the λ parameter the larger the topological instability of a crystalline solid solution. Assuming that a liquid is cooled

---

[*] Corresponding author. Tel.: +55 16 3373 9583; fax: +55 16 3373 9590.
E-mail addresses: falcao@sc.usp.br (M.F. de Oliveira), flavios_pereira@yahoo.com (F.S. Pereira), kiminami@power.ufscar.br (C.S. Kiminami), wjbotta@ufscar.br (W.J. Botta), cbolfa@ufscar.br (C. Bolfarini).

0925-8388/$ – see front matter © 2009 Elsevier B.V. All rights reserved.
doi:10.1016/j.jallcom.2009.10.255

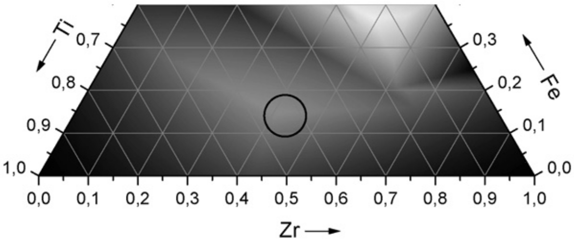

Fig. 1. Plots of minimum topological instability and average electronegativity for Ti–Zr–Fe and Ti–Zr–Co systems. Brighter areas contain the highest product of both factors. Encircled areas show the alloys with the best expected GFA in the Ti–Zr rich side of the diagrams.

fast enough to suppress long range diffusion as well as solute segregation, two choices are possible: polymorphic crystallization of a solid solution (super saturated or not) or amorphous phase formation. If a polymorphic transformation occurs, one would expect a solid solution with the smallest λ among the competing crystalline phases. Based on this assumption, a minimum λ plot is built. The “peaks” on this plot correspond to compositions where the topological instability reaches a local maximum among the surrounding stable phases, and thus a better glass forming ability is expected. Within a given system the highest peaks are the most probable compositions for good glass forming ability.

The topological instability criterion, however, is not the only factor contributing to glass formation. In order to get a more refined method another criterion is taken into account: the average difference in the alloy's electronegativity. The difference in electronegativity among the elements of an alloy is directly related to its formation enthalpy (ΔH) [14] and to the resistance of the glass against crystallization during heating [15]. It is also well known that large negative formation enthalpies among the main constitutive elements are important for glass formation, as was first proposed by Turnbull [16]. Therefore, it is reasonable to suppose that the higher the average difference in electronegativity among the elements the higher the glass forming ability. Thus, like the minimum λ plot, an average electronegativity plot is built for the system of interest. Both these factors are used, assuming a synergistic effect, to produce a final criterion plot. The final plot is thus a simple multiplication of the topological instability and electronegativity criteria.

With regard to average electronegativity, we have introduced and used a modified equation. Following the same idea of a previously introduced equation [14], this new equation is also based on the random packing of neighbors around a central atom. However, we assume that the neighborhood is dependent on the surface concentrations of atoms, instead of simple atomic fractions; in the same way surface concentrations are used for calculations of enthalpies in Miedema's model [17]. Assuming a random distribution of atoms in the alloy, the surface concentration, S_j, of a j atom on the surface of any atom is defined as

$$S_j = \frac{\chi_j . V\mathrm{m}_j^{2/3}}{\sum \chi_j . V\mathrm{m}_j^{2/3}} \qquad (2)$$

where χ_j is the atomic fraction of each element in the alloy and $V\mathrm{m}_j$ is the molar volume.

In the present approach, the surface concentrations are used to weigh the difference in electronegativity between a central atom and its neighbors. Finally, the overall mean is weighted by the atomic fractions of each element, yielding the following equation:

$$\overline{\Delta e} = \sum \chi_i \sum S_j |e_i - e_j| \qquad (3)$$

where $\overline{\Delta e}$ is the average difference in electronegativity, χ_i is the atomic fraction of each element, e_i is Pauling's electronegativity of a central atom i, e_j is the electronegativity of each j neighbor, and S_j is the surface concentration as defined by Eq. (2).

2. Experimental procedure

In addition to the combined topological instability and electronegativity criterium we also have chosen the alloy compositions by evaluating the proximity to a ternary eutectic composition. Four alloy compositions were produced by arc melting of pure elements under argon atmosphere: 1—$Ti_{37.5}Zr_{37.5}Fe_{12.5}Co_{12.5}$, 2—$Ti_{40}Zr_{40}Fe_8Co_{12}$ (close eutectic), 3—$Ti_{43}Zr_{42}Fe_6Co_9$ (close eutectic) and 4—$Ti_{37}Zr_{50}Fe_5Co_8$.

After several runs and remelting procedures in the arc melter, the ingots were sectioned and analyzed by optical microscopy, scanning electron microscopy, X-ray diffractometry and differential scanning calorimetry.

The ingots (1, 2 and 4) were then remelted to produce melt–spun ribbons, which were again characterized by the same techniques just described. One ingot, 3, was remelted and cast into an edge-shaped cavity of a copper mold. The melt–spun ribbons and the edge-shaped cast were analysed by X-ray diffraction. Oxygen content measurements were also performed.

The experimental results were then evaluated in comparison with the theoretical predictions based on the topological instability and electronegativity criteria.

3. Results and discussions

As described earlier, plots of minimum topological instability and average electronegativity were formulated for Ti–Zr–Fe and Ti–Zr–Co, as shown in Fig. 1.

It is important to note that the circles in Fig. 1 show the second best glass forming compositions predicted for both systems. Such compositions were chosen in detriment of the best predicted ones (brighter areas) since the micrographic analyses indicated the presence of ternary eutectic compositions near this encircled areas. Considering that the two plots in Fig. 1 are quite similar in the Ti–Zr rich side of the diagrams, Fig. 2 was plotted to show the compositional range of interest, superimposing the diagrams from Fig. 1. In order to simplify the analysis Fe and Co are assumed to be similar elements, which is consistent with the similarity of both diagrams. Thus, for any composition, the summation of Fe and Co fractions must be considered. In fact, a quaternary plot should be produced in order to show the best fractions of Fe and Co. The open circles in Fig. 2 show a compositional range of 5 at.% around the best predicted GFA compositions in the Ti–Zr rich side of both ternary

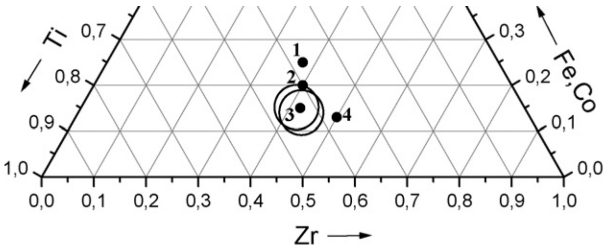

Fig. 2. Plot of experimental points and predicted best GFA compositional range for Ti–Zr rich alloys. The open circles have a radius of 5 at.% around the predicted optimum compositions. Alloys: 1—$Ti_{37.5}Zr_{37.5}Fe_{12.5}Co_{12.5}$, 2—$Ti_{40}Zr_{40}Fe_8Co_{12}$, 3—$Ti_{43}Zr_{42}Fe_6Co_9$ and 4—$Ti_{37}Zr_{50}Fe_5Co_8$.

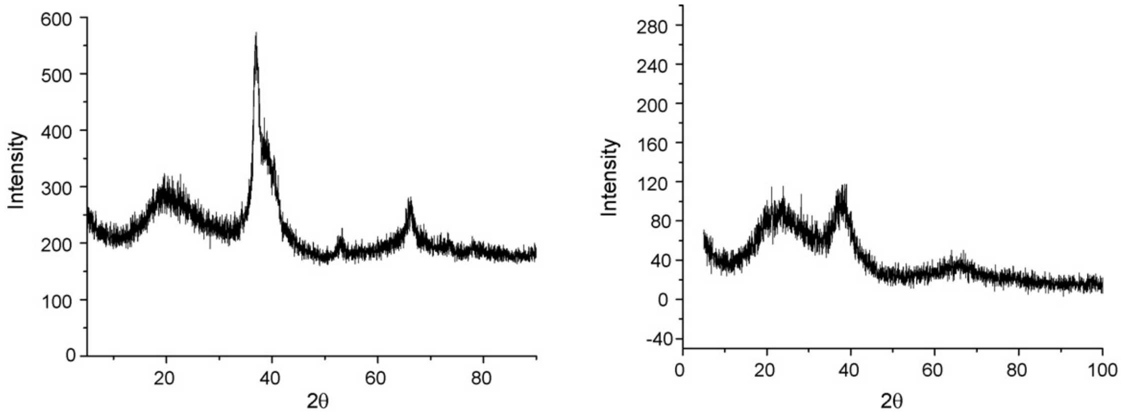

Fig. 3. X-ray diffraction for alloy 1—$Ti_{37.5}Zr_{37.5}Fe_{12.5}Co_{12.5}$ (a) and alloy 2—$Ti_{40}Zr_{40}Fe_8Co_{12}$ (b) melt–spun ribbons.

systems. The point 3, in Fig. 2, is the average position of such best GFA compositions. Furthermore, from Fig. 1 we would expect that Co is more effective to increase the GFA than Fe since the diagram with Co shows brighter areas than that with Fe.

The X-ray diffraction showed that the best GFA among the experimental alloys was the $Ti_{40}Zr_{40}Fe_8Co_{12}$ alloy (point 2) very close to the prediction (point 3) in Fig. 2. This alloy showed the highest fraction of glass in the melt–spun ribbon (see Fig. 3). The $Ti_{37}Zr_{50}Fe_5Co_8$ (point 4) showed a large amount of crystals even in the melt–spun ribbon. The trial to produce some amount of glass by copper mold casting with the best predicted alloy, 3, failed. No amorphous phase could be detected even for a thickness as small as 0.5 mm. The edge shaped cast alloy, 3, was much more contaminated by oxygen, 1500 ppm, than the melt–spun ribbons (1, 2 and 4), 700 ppm. Since the oxygen is a well known trigger for crystallization in Ti and Zr-based alloys the GFA of the alloy 3 could not be compared with alloys 1, 2 and 4.

It is interesting to note that the proposed criterion to select glass former compositions showed that the Ti–Zr rich side of the systems is not the best GFA region. This region should be a second choice but was just chosen because of the results of previous metallographic analysis as already stated. In fact, no melt–spun ribbon was fully amorphous but the criterion predicted that the best glass forming composition found (2) was close to the predicted one (3). Therefore, the experimental results suggest that the proposed criterion is a promising tool for the selection of good glass forming compositions in a given system. Similar analyses of different binary and ternary systems by our research group have pointed in the same direction.

4. Conclusions

The experimental results of glass forming ability in the Ti–Zr rich side of the Ti–Zr–Fe–Co system suggests that combined topological instability and electronegativity criterion is a useful tool to help forecast good glass former alloy compositions in a given system.

The best glass forming Ti–Zr rich alloy was $Ti_{40}Zr_{40}Fe_8Co_{12}$, whose composition closely resembles the one predicted by the combined criterion, $Ti_{43}Zr_{42}(Fe,Co)_{15}$.

Acknowledgements

The authors would like to thank FAPESP and CNPq for financial research support.

References

[1] W.L. Johnson, MRS Bull. 24 (1999) 42.
[2] A. Inoue, Acta Mater. 48 (2000) 279.
[3] W.B. Kim, B.J. Ye, S. Yi, Met. Mater. Int. 10 (2004) 1.
[4] D.E. Polk, A. Calka, B.C. Giessen, Acta Metall. 42 (1971) 530.
[5] C. Suryanarayana, A. Inoue, T. Masumoto, in: H. Kimura, O. Izumi (Eds.), Titanium'80—Science and Technology, The Met. Soc. AIME, Warrendale, PA, 1980, p. 699.
[6] C. Suryanarayana, A. Inoue, T. Masumoto, J. Mater. Sci. 15 (1980) 1993.
[7] L.E. Tanner, R. Ray, Acta Metall. 27 (1979) 1727.
[8] L.E. Tanner, Scr. Metall. 12 (1978) 703.
[9] L.E. Tanner, R. Ray, Scr. Metall. 11 (1977) 783.
[10] C. Suryanarayana, A. Inoue, T. Masumoto, Sci. Rep. Res. Isnt. Tohoku Univ. A28 (1980) 195.
[11] T. Egami, Y. Waseda, J. Non-Cryst. Solids 64 (1984) 113.
[12] R.D. Sá Lisboa, C. Bolfarini, W.J. Botta, F.C.S. Kiminami, Appl. Phys. Lett. 86 (2005) 211904.
[13] C.S. Kiminami, R.D. Sá Lisboa, M.F. de Oliveira, C. Bolfarini, W.J. Botta, Mater. Trans. 48 (2007) (1739).
[14] S.S. Fang, Z.Q. Zhou, J.L. Zhang, et al., J. Alloys Compd. 293–295 (1999) 10.
[15] S.S. Fang, X.S. Xiao, L. Xia, et al., J. Non-Cryst. Solids 321 (2003) 120.
[16] D. Turnbull, J. Chem. Phys. 20 (1952) 411.
[17] F.R. Boer, et al., Cohesion in Metals, 1, North-Holland, 1988.